

LASER INTERFEROMETER GRAVITATIONAL WAVE OBSERVATORY
- LIGO -
CALIFORNIA INSTITUTE OF TECHNOLOGY
MASSACHUSETTS INSTITUTE OF TECHNOLOGY

Technical Note	LIGO-T11XXXXX-vX	2024/08/08
2024 LIGO SURF Interim Report 2: 40m ALS / SFG		
Dhatri Raghunathan		

California Institute of Technology
LIGO Project, MS 18-34
Pasadena, CA 91125
Phone (626) 395-2129
Fax (626) 304-9834
E-mail: info@ligo.caltech.edu

Massachusetts Institute of Technology
LIGO Project, Room NW22-295
Cambridge, MA 02139
Phone (617) 253-4824
Fax (617) 253-7014
E-mail: info@ligo.mit.edu

LIGO Hanford Observatory
Route 10, Mile Marker 2
Richland, WA 99352
Phone (509) 372-8106
Fax (509) 372-8137
E-mail: info@ligo.caltech.edu

LIGO Livingston Observatory
19100 LIGO Lane
Livingston, LA 70754
Phone (225) 686-3100
Fax (225) 686-7189
E-mail: info@ligo.caltech.edu

<http://www.ligo.caltech.edu/>

Contents

1	Introduction	2
2	Theory: Why SFG, calculation of efficiency	2
2.1	LIGO Voyager	2
2.2	Sum Frequency Generation	3
2.3	Calculate single pass efficiency	3
3	SFG Setup at Quantum Interferometry Lab	3
3.1	SHG setup - Cleaning optics and changing mounts	3
3.2	Pump power and beam profile using dataray	5
3.3	Target Beam Waist Estimation	5
4	Mode Matching and Alignment	5
4.1	SHG mode matching	7
4.2	Alignment and observation of SHG	9
5	Characterizing SHG output	9
5.1	Output power as a function of Pump Power	9
5.2	Temperature Readout and Calibration	9

1 Introduction

The LIGO (Laser Interferometer Gravitational-Wave Observatory) detectors are essentially large scale Michelson interferometers which are designed to sense variations in space-time strain induced by passing Gravitational Waves (GWs). The LVK (LIGO-Virgo-KAGRA) detector network currently consists of two Advanced LIGO detectors in the U.S.; the Advanced Virgo detector in Italy; and the Japanese detector, KAGRA. A third Advanced LIGO detector is to be located in India.

The 40m prototype of LIGO at Caltech is a 1:100 scale model of the LIGO facility. It serves as a testing ground for upgrades aimed at enhancing the Advanced LIGO (aLIGO) detectors. The primary objective of this project is to study the implementation of upgrades that significantly improve the sensitivity of the GW detectors. Currently, the detector faces challenges related to quantum efficiency (QE) in photodetection and laser feedback stabilization.

During this phase of my project, I have focused on the SFG - ie. Sum Frequency Generation aspect. The objective is currently to demonstrate and characterize single pass Sum Frequency Generation in the Quantum interferometry lab.

2 Theory: Why SFG, calculation of efficiency

2.1 LIGO Voyager

The future upgrade to LIGO ie. Voyager's high frequency sensitivity is achieved with high power operation and substituting unsqueezed vacuum fluctuations with a highly squeezed vacuum state. Any losses in the system provide a path for unsqueezed vacuum to couple to the readout, with small losses significantly degrading the squeezed state. Therefore, the squeezing loss budget is very strict. For the readout photodetectors (PDs), this includes a maximum allowable loss of 1%, implying very high ($\geq 99\%$) quantum efficiency (QE) at the 2 μm operating wavelength. Direct detection of IR radiation is possible with PIN junction photodetectors made from HgCdTe and InAsSb. The maximum demonstrated QE of these detectors is of the order of 90% and will need improvement for use in Voyager.

Sum-frequency generation (SFG) provides an alternative path for high QE photodetection. By mixing a strong (e.g. resonantly enhanced) pump, for example at 1064 nm, the 2 μm fields may be upconverted to 700 nm. After upconversion, traditional InGaAs or Si PDs may be used to achieve $\geq 99\%$ QE. Light upconversion for improved photodetection. In the case of resonant SFG, even a modest finesse (< 1000) cavity providing optical gain for the pump wavelength may reach a quantum efficiency of $\geq 95\%$. With further R&D, such upconversion quantum efficiencies may approach $\geq 99.9\%$, matching external QE values attainable with Si devices.

2.2 Sum Frequency Generation

Crystal materials lacking inversion symmetry can exhibit a so-called nonlinearity. In such nonlinear crystal materials, second order effects such as Sum Frequency Generation ie. SFG, or difference frequency generation ie. DFG can occur, where two pump beams generate another beam with the sum or difference of the optical frequencies of the pump beams. Second order nonlinear processes require phase matching to be efficient. Usually there is no simultaneous phase matching for multiple processes, so that only one of them can take place.

SFG is a parametric process, meaning that the photons satisfy energy conservation: $\omega_3 = \omega_1 + \omega_2$, where ω_3 is the sum frequency (SF) and ω_1, ω_2 are the fundamental pump frequencies. Voyager uses a signal of 2 μm , so at the output of the GW detection, the pump used will be a 1064-nm Nd:YAG laser, resulting in an upconverted signal output at 700 nm.

A special case of sum-frequency generation is second-harmonic generation, in which $\omega_1 = \omega_2$. This has been done before at the Quantum Interferometry Lab, where I am working on replicating it to practice alignment because in second-harmonic generation, only one input light beam is required. If $\omega_1 \neq \omega_2$, two simultaneous beams are required, which can be more difficult to arrange at the outset.

2.3 Calculate single pass efficiency

The efficiency of the conversion process for a waveguide of length L with negligible propagation loss and a phase-matched interaction is given by

$$\eta = \sin^2 \left(\sqrt{\eta_{\text{nor}} \cdot P_p \cdot L} \right)$$

where P_p is the pump power. The normalized efficiency η_{nor} is given by

$$\eta_{\text{nor}} = \frac{\varepsilon_0^2 \cdot d_{\text{eff}}^2 \cdot |\theta_Q|^2 \cdot 2\omega_1\omega_2 \cdot Z_0^3}{n_1 \cdot n_2 \cdot n_p}$$

where d_{eff} is the effective nonlinear coefficient, $Z_0 = \sqrt{\frac{\mu_0}{\varepsilon_0}}$ is the impedance of free space, n_j are the effective indices of refraction, and θ_Q is the mode-overlap integral for three-wave interactions.

I wrote a python code to compute this efficiency as a function of pump power as shown in fig. 1.

3 SFG Setup at Quantum Interferometry Lab

3.1 SHG setup - Cleaning optics and changing mounts

The Second Harmonic Generation (SHG) setup was initially configured by another lab member Shoki. This involved a single laser of wavelength 1064 nm as input to a PPKTP crystal, observing an SHG output of 532 nm light.

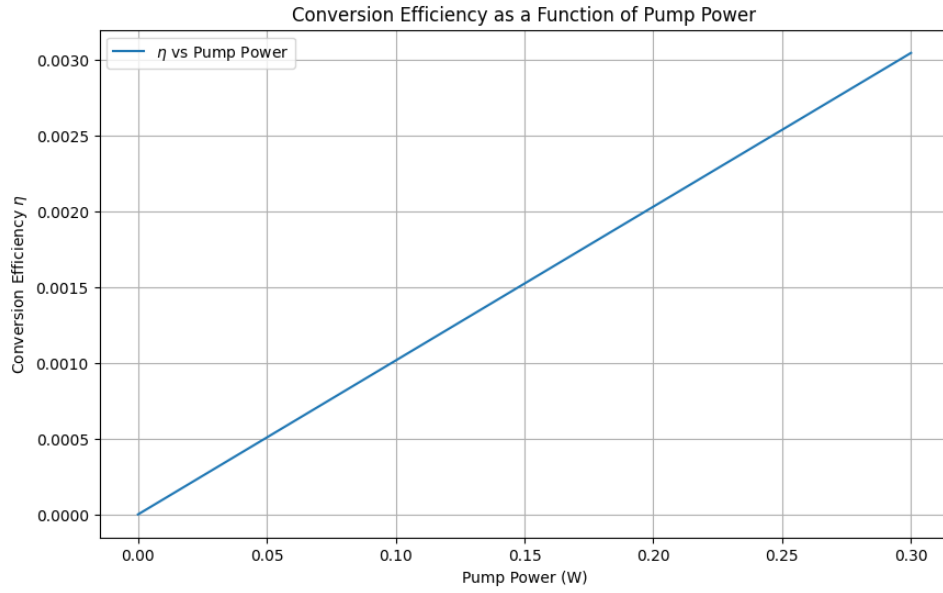


Figure 1: Efficiency as a function of pump power. Through the function is a sine squared, it is linear at low power.

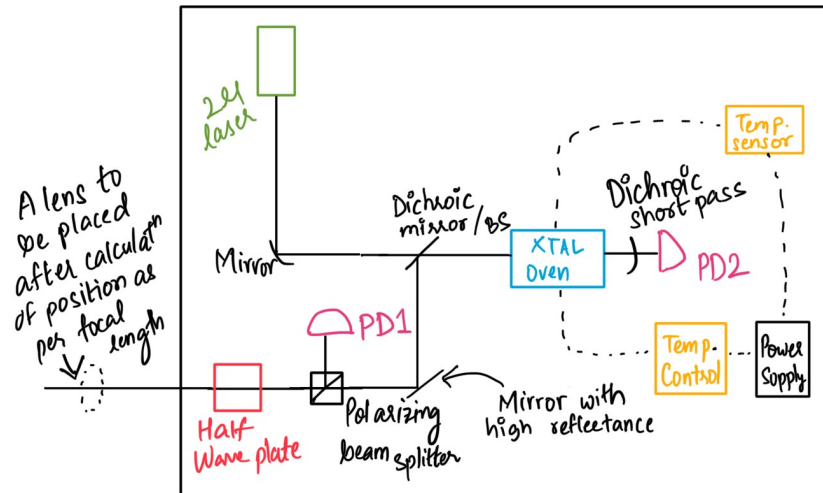


Figure 2: Schematic for the setup to observe Sum Frequency Generation

Using this as a basis, I drew up a schematic (fig. 2) for Sum Frequency Generation. The pump (1064 nm) will be the same one currently in use for the SHG - a Diabolo Laser. It is placed on the other side of the table where the setup for another experiment ie. WOPA is. After clearing the table of other unused mounts and optics, I cleaned the SHG related optics using Isopropyl alcohol and changed the first mirror mount to a transparent one that allowed me to see if the beam was centered and aligned before sending it to the other side of the table.

3.2 Pump power and beam profile using dataray

The 1064 nm laser beam power and beam profile were measured using a DataRay beam profiler. Laser power was measured at three different points and found to be as follows:

- Before the half-wave plate: 309 mW
- After the polarizing beam splitter on the WOPA side: 9 mW
- After the polarizing beam splitter on the SFG side: 300 mW

The beam profiler initially faced issues detecting the cameras, but this was resolved by rebooting the laptop and the DataRay application. The beam was found to be diverging, with the beam waist appearing to be inside the Diabolo box. To accurately determine the beam waist and its position, I fitted the beam width data to a hyperbolic model. In this model, the horizontal axis (x) represents the distance from the laser (Rayleigh range) and the vertical axis (y) represents the beam width. The hyperbolic equation used is:

$$y = b^2 + \left(\frac{x}{z_0}\right)^2$$

where b is the beam waist, and z_0 is the Rayleigh range.

The beam width data was used to fit the hyperbola, assuming the initial beam waist was positioned at the laser (i.e., $x = 0$), as shown in Fig. 3. The fitted hyperbola indicated an initial beam waist of approximately 0.9 mm.

3.3 Target Beam Waist Estimation

The PPKTP crystal damage threshold at 1064 nm is 260 MW/m². To ensure safe operation, the target beam waist was estimated, keeping in mind the crystal damage threshold and the oven opening size. Figure 4 is a plot of the minimum beam waist as a function of pump power, which indicates that a beam waist above 25 microns would be safe for the crystal.

4 Mode Matching and Alignment

Beam Width in X and Y directions vs. Distance Fitted with Hyperbola: $\frac{x^2}{a^2} - \frac{y^2}{b^2} = 1$

x and y are the Rayleigh range and beam width respectively.

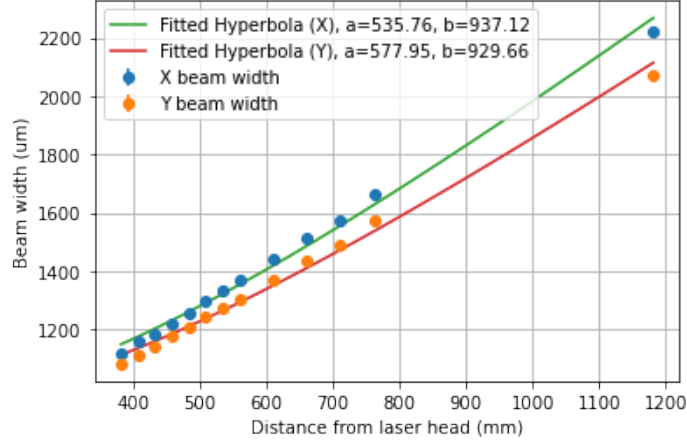


Figure 3: Fitting of beam width data to a hyperbolic model.

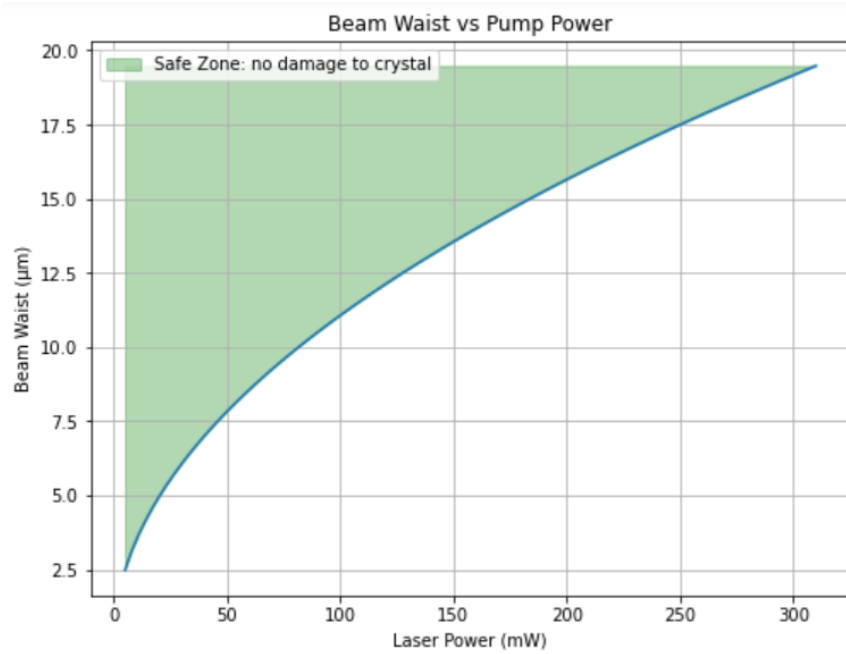


Figure 4: Minimum (safe) beam waist as a function of pump power.

4.1 SHG mode matching

Mode matching was conducted to achieve the desired beam waist at the oven position (87-88 inches from the laser). The q parameter is a complex number that describes the beam's curvature and spot size at a given point. For a Gaussian beam, the q value at any position z can be expressed as:

$$q(z) = z + iz_0$$

where z_0 is the Rayleigh range, which is related to the beam waist w_0 by:

$$z_0 = \frac{\pi w_0^2}{\lambda}$$

After calculating the initial and target q values using the corresponding beam waist values and positions, the ABCD matrix equation for transformation can be written out and calculated to find the positions of the lenses to be used. For a system of multiple lenses and free space propagation, the overall ABCD matrix is the product of individual matrices.

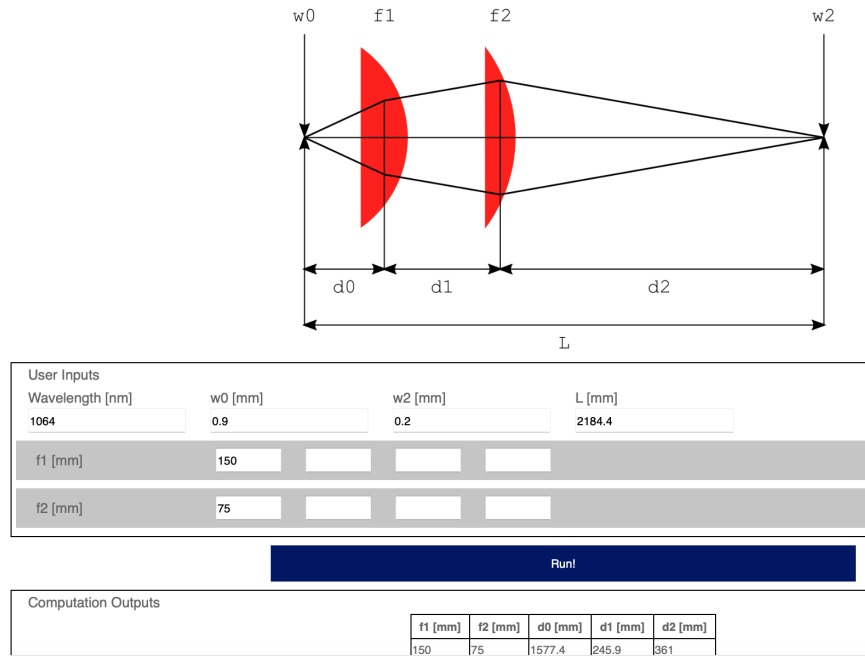


Figure 5: Mode matching using 2 lenses to estimate the positions of the lenses and get the required waist at the oven

Using an online Mode-Matching Calculator as shown in fig. 5, I procured an initial estimate of the lens positions. After testing various lens combinations, lenses with focal lengths of 150 mm and 75 mm were selected. However, there was a power loss of 20% detected due to the 150 mm lens, so I replaced it with a 175 mm lens to minimize power loss till another 150 mm lens was found. The waist was further decreased to about 80 micron by changing the lens positions. The beam was profiled again and the gaussian beam fit is shown in fig. ??.

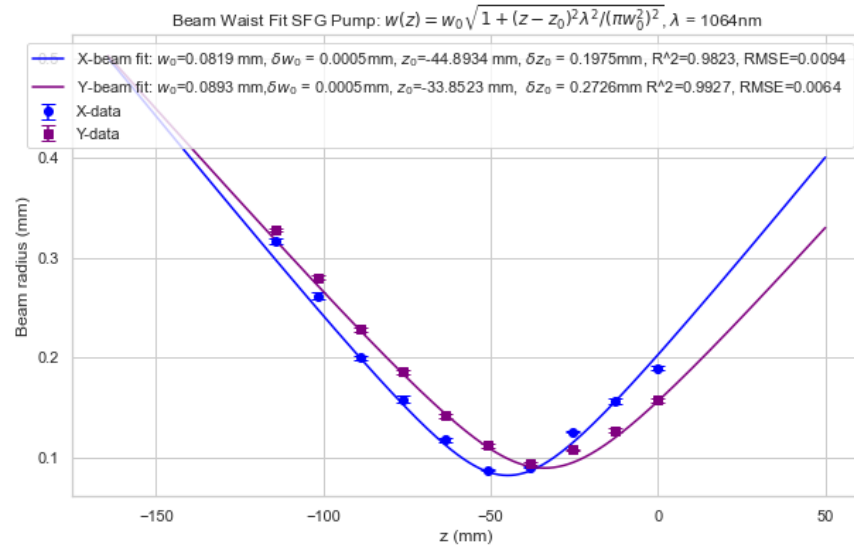


Figure 6: Gaussian beam fit after placing lenses to achieve mode matching

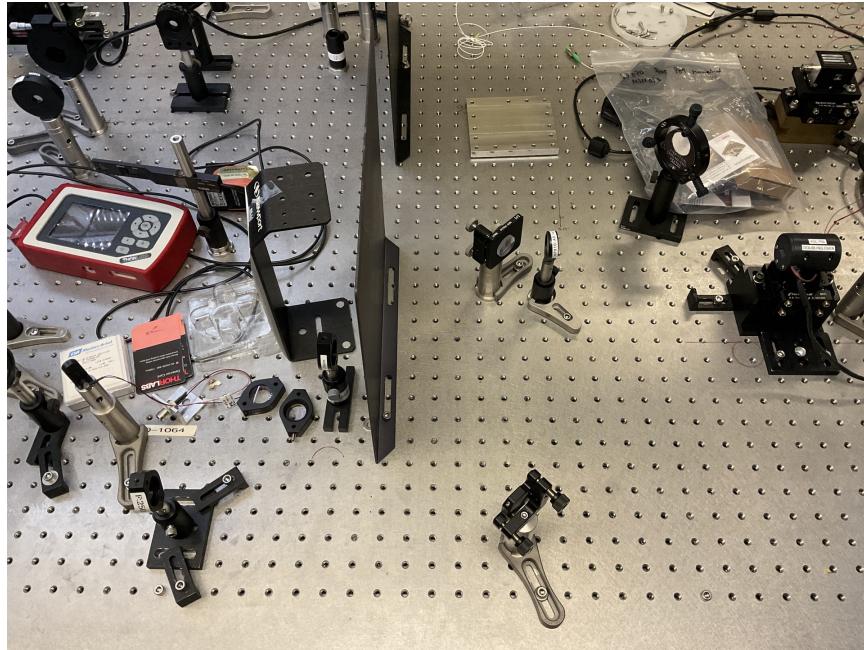


Figure 7: Mode matched and aligned SHG setup achieved

4.2 Alignment and observation of SHG

Alignment was achieved using two steering mirrors to control the two parameters - beam's incidence angle and position on the crystal. The final lens positions were: $f = 250$ mm at 36.5 inches and $f = 150$ mm at 63 inches from the laser head. The setup is shown in fig. 7

I placed a dichroic beam splitter after the crystal oven, which was reflective to 1064 nm and transmissive to 532 nm. A photodetector PDA10A was also placed to detect the green light at the output.

5 Characterizing SHG output

5.1 Output power as a function of Pump Power

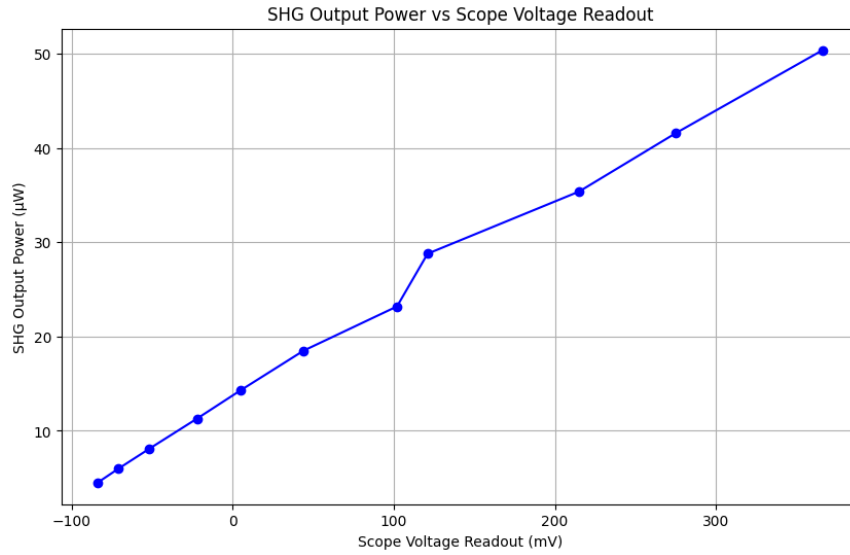


Figure 8: Oscilloscope Voltage to Output Power calibration.

Voltage that we read out on the oscilloscope connected to the PD corresponds to the output power at that point. This was calibrated and the plot is shown in fig. 8

The SHG output power has correlation with the pump power. Measuring this output power as a function of input pump power gives us information which we can use to optimize the upconversion efficiency. The pump power was changed using the half wave plate and the output power was measured on the oscilloscope as volts. The plot is shown in fig. 9

5.2 Temperature Readout and Calibration

Given the inaccuracy of the oven controller readout, three robust temperature readout methods were explored: 1. A sensor consisting of a complex circuit 2. Thorlabs TED200C 3. A resistor-based readout

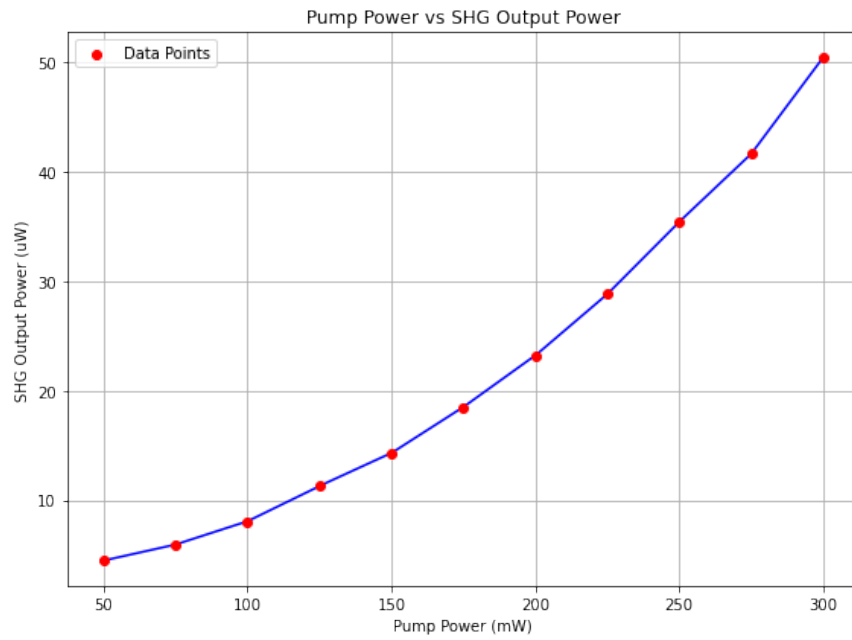


Figure 9: SHG output Power as a function of pump power.

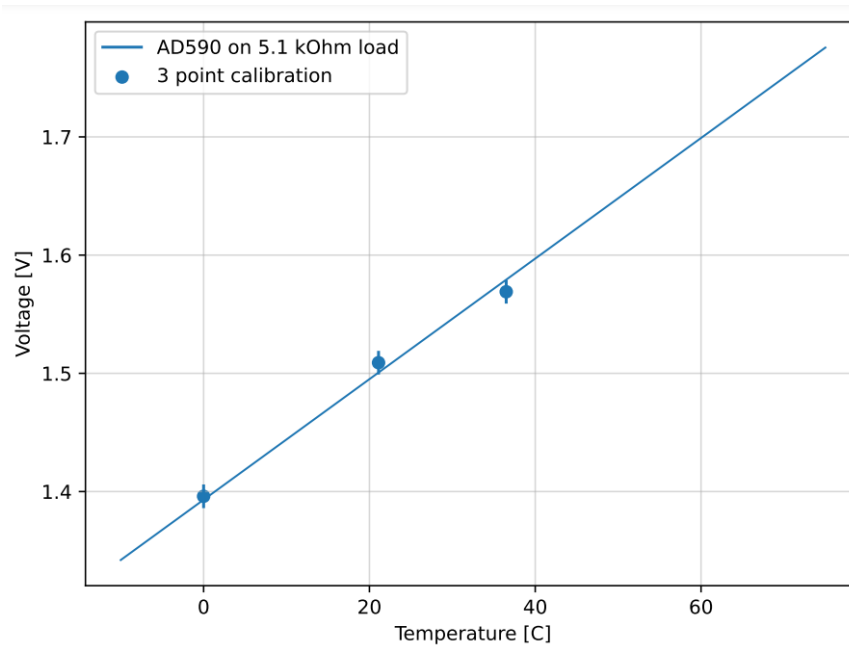


Figure 10: Calibration curve for the temperature readout, assuming 0.2 error in room and body temperatures.

After spending a while trying to configure the other options, finally a simple temperature readout setup was implemented using a 5.1 K Ohm resistor, which was then calibrated using 3 temperature points of reference. The calibration curve for the readout is shown in fig. 10

References

- [1] A Cryogenic Silicon Interferometer for Gravitational-wave Detection, <https://arxiv.org/pdf/2001.11173>
- [2] Long-wavelength-pumped upconversion single-photon detector at 1550 nm: performance and noise analysis, <https://opg.optica.org/oe/fulltext.cfm?uri=oe-19-22-21445&id=223665>
- [3] Improvement to Sellmeier equation for periodically poled LiNbO3 crystal using mid-infrared difference-frequency generation, <https://www.sciencedirect.com/science/article/pii/S0030401806006778>